THE IMPACT OF THE FRACTURING ADDITIVES ON THE SHEAR RATE IN THE FRACTURE DURING FRACTURING TREATMENT

Aymen Al-Ameri
Texas Tech University
Bob L. Herd Department of Petroleum Engineering

ABSTRACT

During hydraulic fracturing treatment, low shear rates in the fracture are desired to keep higher fluid viscosity and to reduce the effect on the filter cake. The majority of the literature assumes a shear thinning behavior for the polyacrylamide polymer solution at low shear rates. The objective of this study is to investigate the effect of the fracturing additives (friction reducer, guar, potassium chloride, breakers, crosslinkers, and surfactants) on the in fracture- shear rate using experimental and analytical study.

For slickwater fluids, the effect of the KCl content on the fluid shear behavior was investigated at different friction reducer concentrations. On the other hand, ten gelled fluids were prepared to study the effect of the gelling agent (guar) and the other fracturing additives concentration on the fluid shear rate.

A rotational Viscometer was used to measure the viscosity of the slickwater fluids at surface conditions for a wide range of shear rates. Moreover, the changes in flow behavior and consistency indexes (n & k) of the gelled fluids as a function of time are measured at numerous temperatures.

A new equation was derived to predict the fluid shear rate in the fracture at any time during fracturing treatment. The main parameters of the equation are; shear rate independent fracture width (derived in this study) and (n & k).

The Viscometer study results showed that KCl free Slickwater fluids are always behave as shear thinning fluids regardless of the friction reducer concentration. Adding KCl to the fluids lead to the presence of shear thickening behavior at low or medium shear rates.

The analytical model results showed that the shear rate in the fracture depends on fracturing additives concentration and the formation temperature. The shear rate in the fracture is proportional to the concentration of the gelling agent and inversely proportional to crosslinker concentrations. Adding breaker to the fluid increases the shear rate while the non-ionic surfactant leads to decrease the shear rate. Moreover, the shear rate increases as the formation temperature increases.

INTRODUCTION

During fracturing treatment, different types of chemical additives are used to provide a set of properties of the fluid. Friction reducers which are polyacrylamide-based- polymer are added to water to manufacture slickwater fracturing fluid. They reduce the friction generated as the fluid is pumped down the well tubular. The gelling agents such as Guar gum which is a naturally occurring polysaccharide is used to increase the viscosity of the fracturing fluid and that provide better proppant carrying ability and fluid loss control (Gall and Raible 1985). Accordingly, the most essential property of the injected polymer solution is its highly non-Newtonian viscosity that reflects a viscosity dependence on flow or shear rate being either shear thinning or shear thickening. On the other hand, chemical breakers are added to reduce the molecular weight of the polymers (Weaver et al., 2003) and thereby; reducing fluid viscosity, and this facilitates the flowback of the residual polymer.

The rheology of the polymer plays a very important role in determining injectivity, fracture growth and hydrocarbon recovery. For the shear-thinning polymer, the fracture does not grow as much as in the case of a viscoelastic fluid (Zechner et al. 2013). In the fracture, the approximate shear rate can be as low as (30-50 sec^{-1}) causing the fluid to have a high viscosity but for some soft rock treatments the shear rate may be much lower than this, and in some hard rock treatments, the shear rate may be much greater (Carl Montgomery 2013).

Because of the polymer complex rheology, the literature showed a variety of flow behavior for the polymer solutions. Biopolymers show shear thinning behavior when characterized with a rheometer or when injected into a core plug representing porous media (Hirasaki and Pope 1974, Hill et al. 1974, Chauveteau and Kohler 1984, Cannella et al. 1988). Polyacrylamide solutions show shear thinning behavior at low shear rates that becomes shear thickening behavior above a characteristic flow velocity (Seright 1983, Maerker and Sinton 1984 and Delshad 2008). In many reservoir simulators (Bondor et al. 1972; Todd and Chase 1979), the polymer solution was assumed to behave as a shear thinning (pseudoplastic) non-Newtonian fluid. Zechner et al. 2013 had done a pilot test to recognize the difference in the rheology results measured using the rheometer and the viscosity determined from polyacrylamide polymer flooding in core samples. The results of the rheometer for a (1 ppt) polymer solution prepared with an artificial field brine showed only a shear thinning behavior. While the injection results of the same polymer solution into a core plug showed a shear thickening behavior at less than (15 m /d). Velocities and a shear thinning behavior at higher velocities. The shear thinning behavior was attributed to the polymer degradation.

The work of Gall and Raible (1985) showed that the polymer thermal degradation depends on polymer type, breaker type and concentration, reaction time, temperature, and the presence of fluid constituents (salts, crosslinkers, acids, etc.). Nasr-El-Din et al. (2007) studied the degradation of guar based, borate crosslinked gels. Their work showed that the gel degradation time is a function of breaker type, concentration, and the polymer concentration. The viscosity measurements of Sarwar et al. (2011) showed that the reduction in the gel viscosity depends on both the breaker. In general, if a fracturing fluid retains 50-100 cp viscosity (at reservoir temperature and a shear rate of 170 sec^{-1}) at the end of the fracture treatment, it will provide essentially perfect proppant transport (Nolte, 1982).

Fracturing fluids are non- Newtonian shear thinning fluids; moreover, the power law equation is widely used to model the viscous behavior of this kind of fluids. The Most fracturing service companies describe the viscous behavior of their fluids concerning the power law flow behavior and consistency indexes (n & k). The values of (n & k) for the various fluid systems are published for a range of time-temperature conditions. The problem, however, has been that the values of (n & k) for any given fluids are functions of the mixing and testing procedure. Therefore, it has always been difficult for independent laboratories to either reproduce the data from a given service company or to meaningfully compare the published data between any two service companies. (Worlow 1989).

FLUIDS PREPARATION

Model 20 constant speed blender manufactured by OFITE was used in preparing the fluids used in this study, Figure 1.

The blender facilitates the preparation of fracturing fluids for testing according to API guidelines, and it also provides a means of consistently preparing fracturing fluids. The blending speed used in preparing the fluids of this study is 1000 RPM.

FLUIDS VISCOSITY MEASUREMENTS

The used Viscometer is a fully automated system for measuring fluid viscosity at shear rate range (0.01-1700 sec^{-1}) and temperatures up to 200 ºF, Figure 2.

The viscometer uses a rotating cup and a stationary bob with a gap between the two that simulates the fracture, Figure 3.

The viscometer is connected to the computer for an automatic data acquisition. The viscometer was used to measure the viscosity of the slickwater fluids at surface conditions for a wide range of shear rates. Moreover, it was used to measure the changes in (n and k) due to the polymer degradation of the gelled fluids as a function of time and at temperatures (180, 150, 120 and 100 Fahrenheit).

EFFECT OF POTASSIUM CHLORIDE ON THE SHEAR RATE OF FRICTION REDUCER FLUIDS

The friction reducer fluids with the shear thinning behavior tend to have high viscosities at low shear rates and that is important for better proppant carrying ability and fluid loss control.

Friction reducer fluids are commonly used in the pad stage of the fracturing treatment. Friction reducer is a polyacrylamide-based polymer with molecular weigh about (2000000). To study the flow behavior of the polyacrylamide solutions, friction reducer with concentrations 0.05%, 0.1% and 0.15% were added to the base fluid which is distilled water. The apparent viscosity and the shear rates were measured for a wide range of shear rates as shown in Figures 4 and 5.

The results show that all fluids have a shear thinning behavior even for low shear rates.
Potassium chloride is added to the fracturing fluid as a clay stabilizer. In this study, the effect of the KCl concentration on the friction reducer fluid flow behavior is investigated. The investigated KCl concentrations are (1%, 3%, 5% and 7%). Figures 6 through 9 show the viscosity measurements as a function of the shear rate.

The main results can be summarized as follow:

- Adding KCl lead to the presence of shear thickening behavior at low or medium shear rates depending on the friction reducer concentration.
- The more KCl content in the friction reducer fluid, the less fluid viscosity (more fluid loss and less pump pressure). Accordingly, optimum concentration of KCl should be considered.
- Friction reducer concentration less than 0.1% is not recommended at KCl content less than 2% since it leads to either shear thickening or Newtonian flow behaviors at high shear rates.
- KCl concentrations more than 3% lead to increase the shear thickening interval.
- KCl concentration of 3% is recommended.

GELLED FLUID- POLYMER THERMAL DEGRADATION

In this study, the changes in the (n & k) indexes due to the polymer thermal degradation are measured experimentally as a function of time. The measurements include linear and crosslinked fluids and at temperatures (180 ^oF, 150 ^oF, 120 ^oF and 100 ^oF). The results are used to verify the new suggested equations for the shear rate in the fracture.

Gelled Fluids

The gelled fluids are prepared as two groups of a wide range of additives concentration (Kelvin Nder Abba 2016). Group1 represents low additives concentration gelled fluids, Table 1 while group2 is for the high additives concentration gelled fluids, Table 2.

The Experiment Results of the Viscosity Measurements

The indexes (n & k) are measured as a function of time using rotational speeds (300 and 600 rpm). Therefore, the fluid viscosity is measured at different shear rates using the power law equation.

$$\mu = k\,\gamma^{n-1} \quad (1)$$

The viscosity measurements for non-crosslinked fluids at a shear rate of 511 sec^{-1} and temperatures 180 ^oF, 150 ^oF, 120 ^oF and 100 ^oF are shown in Figures 10 through 17.

The figures show that the main loss in the viscosity takes place during the fluid heating up process that takes place in the wellbore and the fracture. The measurements show that the fluid thermal degradation is much reflected by the degradation of the consistency index (k) and the slight increase of flow behavior index (n).

For temperatures greater than 150 ^oF, the fluids degrade very rapidly; so, it is recommended to use less concentration of breaker or to use another type of the breaker like encapsulated oxidative breakers. Generally, adding non-ionic surfactant to the fluid leads to increase the viscosity. It is worth noting that at temperature 100 ^oF, Fluid1 and Fluid6 (guar only) degrade earlier than the other fluids and adding breaker enhances the viscosity.

Since the shear rate of the crosslinked fluids in the fracture is low (Worlow 1987), the viscosity of the crosslinked fluids was measured experimentally at a shear rate of 50 sec^{-1}. The viscosity measurements were at temperatures 150 ºF, 120 ºF and 100 ºF as shown in Figures. 18 and 19. For temperatures greater than 150 ºF, the crosslinker has no effect to stabilize the viscosity because of the breaker effect.

SHEAR RATE IN THE FRACTURE DURING FRACTURING TREATMENT

Low shear rates during fracturing treatment are recommended to keep higher fluid viscosity and reduce the effect on the filter cake and thereby; enhancing the fluid proppant carrying ability and reduced the fluid loss into the formation.

The shear rate profile in a Rectangular conduit:

$$\gamma = \frac{\partial v(y)}{\partial y} = -\frac{1}{2\mu}\frac{\partial p}{\partial L}(w-2y) \qquad (2)$$

if y=0 (fracture wall), the shear rate is maximum.

if y=w/2 (fracture center), the shear rate is (0). For an average shear rate in the fracture, y is assumed to be equal to w/4. Therefore, equation 2 can be written as:

$$\gamma = \frac{\partial v(y)}{\partial y} = -\frac{1}{\mu}\frac{\partial p}{\partial L}\, w \qquad (3)$$

Substituting Eq. 1 in Eq. 3 yields:

$$\gamma = -\frac{1}{k\,\gamma^{n-1}}\frac{\partial p}{\partial L}\, w \qquad (4)$$

Solving for the shear rate:

$$\gamma^n = -\frac{1}{k}\frac{\partial p}{\partial L}\, w \qquad (5)$$

The pressure-drop resulting from the flow of Power Law fluids through parallel plate (Economides and Nolte 2010):

$$\frac{\partial P}{\partial L} = \left(\frac{4n+2}{n}\right)\frac{2\,q^n k}{h_f^n\, w^{2n+1}} \qquad (6)$$

Substituting Eq. 6 in Eq. 5 yields:

$$\gamma^n = -\left(\frac{4n+2}{n}\right)\frac{q^n}{h_f^n w^{2n}} \qquad (7)$$

Re-arranging Eq. 7:

$$\gamma = \left[-\left(\frac{4n+2}{n}\right)\left(\frac{q}{10.686\, h_f}\right)^n\left(\frac{12}{w}\right)^{2n}\right]^{1/n} \qquad (8)$$

or

$$\gamma = -13.476\left(\frac{4n+2}{n}\right)^{\frac{1}{n}}\frac{q}{h_f\, w^2} \qquad (9)$$

Eq. 9 is a function to the flow behavior index and the fracture width which is in turn function to the consistency index. Accordingly, the effect of the fluid thermal degradation is represented by the fracture width. Moreover, the equation shows that the shear rate increases down the fracture towards the fracture tip because of the reduction in the fracture width. In this study, new equation is developed to calculate (w) in Eq. 9 which is the shear rate independent fracture width.

SHEAR RATE INDEPENDENT FRACTURE WIDTH

The net pressure in the fracture is (Economides and Nolte 2010):

$$P_{net} = \frac{w\,E'}{4\,L_f} \qquad (10)$$

Integrating Eq. 6 yields:

$$P_{net} = \left(\frac{4n+2}{n}\right)\frac{2q^{n}k\, L_f}{h_f^{n} w^{2n+1}} \tag{11}$$

Combining Eq. 10 and Eq. 11 yields:

$$\frac{w\, E'}{4\, L_f} = \left(\frac{4n+2}{n}\right)\frac{2q^{n}k\, L_f}{h_f^{n} w^{2n+1}} \tag{12}$$

Re-arranging Eq. 12 for the fracture width:

$$w^{2n+2} = \left(\frac{4n+2}{n}\right)\frac{8q^{n}k\, L_f^2}{h_f^{n} E'} \tag{13}$$

The volume of fluid in the fracture in both wings (Economides and Nolte 2010):

$$q.t = 2h_f L_f w \tag{14}$$

Re-arranging Eq. 14 for the fracture length:

$$L_f = \frac{q\, t}{2h_f\, w} \tag{15}$$

Substituting Eq. 15 in Eq. 13 and re-arranging for fracture width:

$$w_0 = 12\left[1.04\left(\frac{4n+2}{n}\right)\left(\frac{q}{10.686\, h_f}\right)^{n+2}\frac{k_p}{E'}\; t^2\right]^{\frac{1}{2n+4}} \tag{16}$$

if n=0, the exponent $\frac{1}{2n+4}$ would be equal to $\frac{1}{4}$
if n=1, the exponent $\frac{1}{2n+4}$ would be $\frac{1}{6}$
Accordingly, the exponent $\frac{1}{2n+4}$ can be reduced to $\frac{1}{5}$, thereby; n=0.5

Eq.16 can be rewritten as:

$$w_0 = \left[5549\left(\frac{q}{h_f}\right)^{2.5}\frac{k_p}{E'}\; t^2\right]^{\frac{1}{5}} \tag{17}$$

or:

$$w_0 = 5.61\left(\frac{q}{h_f}\right)^{\frac{1}{2}}\left(\frac{k_p}{E'}\right)^{\frac{1}{5}}\; t^{\frac{2}{5}} \tag{18}$$

Eq.18 is independent of the shear rate; moreover, the effect of the fluid thermal degradation is represented by an explicit function to the consistency index instead of the viscosity as in the case of the available analytical models (PKN, KGD, Nordgren) to calculate fracture width.

VERIFICATION OF THE SHEAR RATE INDEPENDENT FRACTURE WIDTH EQUATION

To verify the results of Eq.18, the data in Table 3 are used to calculate the fracture width with and without considering the effect of the fluid thermal degradation. The calculated fracture width at temperature 120 ^{o}F are shown in Figures. 20 through 25. Moreover, the figures present the calculated fracture width using Nordgren's equation for the case of considering fluid thermal degradation.

The figures above show that the fracture width calculated from the new shear rate independent equation (coarse dotted line) is more sensitive to the fluid thermal degradation than the fracture width calculated from the Nordgren's equation (solid line) at a shear rate 170 sec^{-1}. Therefore, the new equation indicates the advantage of using the consistency index over the viscosity to reflect the fluid thermal degradation. Moreover, the fluid thermal degradation at temperatures exceeds 120 ^{o}F lead to a significant reduction in the fracture width in comparison with the case of ignoring the effect of the fluid thermal degradation (fine dotted line). The fracture width difference between the case of ignoring the thermal degradation and the case of considering it, after five hours of the fluid thermal degradation is shown in Table 4.

THE SHEAR RATE IN THE FRACTURE DURING FRACTURING TREATMENT

Substituting Eq. 18 into Eq. 9 yields;

$$\gamma = -4.578\left(\frac{4n+2}{n}\right)^{\frac{1}{n}}\left(\frac{E'}{k_p}\right)^{\frac{2}{5}} t^{-\frac{4}{5}} \qquad (19)$$

Eq. 19 shows that the shear rate in the fracture throughout fracturing treatment is independent of the fluid pumping rate and fracture height. Moreover, the effect of the fluid thermal degradation is represented by an explicit function to the consistency index.

The results of the calculated shear rates using either Eq. 9 or Eq. 19 after one hour and two hours of the fluid thermal degradation at temperatures 100 ^oF and 120 ^oF are shown in Tables 5 and 6 respectively.

The results show that the value of the shear rate in the fracture depends on the fracturing additives concentration and the formation temperature. Accordingly, the shear rate in the fracture could reach high values (>>100 sec^{-1}). Worlow (1987) showed that the fracturing fluid throughout the fracturing treatment is subjected to low shear rates in the fracture.

It is important to optimize the fracturing additives for the concept of a low shear rate in the fracture (<100 sec^{-1}) for better proppant transportation and less fluid loss. The above tables show that the shear rates of Fluid6 is significantly higher than the shear rate of Fluid1. The reason is that for linear non-crosslinked fluids, as the gelling agent concentration increases, the flow behavior index decreases while the consistency index is slightly increases (<1). Therefore, for linear non-crosslinked fluids, the shear rate controlling factor is the flow behavior index.

The crosslinked fluids show less shear rate in comparison with the non-crosslinked fluids (Fluid1 and Fluid6). The reason is attributed to the high values of the consistency index (>>1) when crosslinkers are added to the fluid. Therefore, for crosslinked fluids, the shear rate controlling factor is the consistency index.

The breakers in both non-crosslinked fluids and crosslinked fluids lead to increase the shear rate because it reduces the consistency index.

The non-ionic surfactant leads to decrease the shear rate since it increases the consistency index of the degraded fluids (fluid 5 and fluid 10).

Generally, as the temperature increases, the consistency index decreases and the flow behavior index increases. As an integrated effect, the shear rate is increased.

CONCLUSIONS

1. KCl free friction reducer fluids always show shear thinning behavior at low and very low shear rates
2. Adding KCl to the friction reducer fluid leads to present a shear thickening behavior at low or medium shear rates followed by a shear thinning behavior.
3. The thermal degradation of fluids with a wide range of fracturing additives concentration is evaluated by measuring the changes in the power law flow behavior and consistency indexes as a function of time. The results show that the fluid thermal degradation leads to significant reduction in the consistency index and a slight increase in the flow behavior index.
4. The shear rate during fracturing treatment is an important aspect in optimizing fracturing additives concentration. It is important to keep low shear rates during fracturing treatment in order to enhance the fluid proppant carrying ability and reduce the fluid loss into the formation.
5. An equation to calculate the shear rate in the fracture during fracturing treatment is developed. The equation is independent of fluid pumping rate and fracture height. Moreover, the equation shows that the shear rate in the fracture depends on the integrated effect of flow behavior index and the fracture width which in turn depends on the consistency index. The equation can also be used to calculate the viscosity in the fracture during the fracturing treatment.
6. Shear rate independent equation to calculate the fracture width is developed. In comparison to Nordgren's equation, the new equation seems to be more sensitive to the fluid thermal degradation. Moreover, the thermal degradation has a significant effect on the fracture width for temperatures more than 120 ^oF.
7. The shear rate of the non-crosslinked fluids increases as the concentration of the gelling agent

increases. For crosslinked fluids, as the gelling agent, crosslinker and non-ionic surfactant increase, the shear rate decreases. While adding more breaker concentration increases the shear rate values. Moreover, the shear rate is proportional to the formation temperature.

8. The shear rate increases gradually away from the hydraulic fracture mouth and reaches its maximum value at the tip of the fracture when the width value approaches the minimum.

NOMENCLATURE

English Symbols

h_f	=	fracture height, ft
k	=	power law consistency index, Pascal.sec^n
k_{wi}	=	water consistency index before polymer solution injection, Pascal.sec^n
k_p	=	polymer solution (fracturing fluid) consistency index, Pascal.sec^n
L_f	=	fracture length, ft
n	=	power law flow behavior index
P_{net}	=	net pressure in the fracture, psi
q	=	injection rate, bbl/min
t	=	time, minute
w	=	capillary tube or fracture width, inch
w_o	=	fracture width at the wellbore, inch
W	=	capillary tube maximum width, inch

Greek Symbols

$\frac{\partial P}{\partial L}$	=	power law pressure drop, psi/ft
E'	=	plain strain modulus, psi
γ	=	shear rate, sec^{-1}

REFERENCES

1. Bondor, P. LK., Hirasaki, G. J. and Tham, M. J. 1972. Mathematical Simulation of Polymer Flooding in Complex Reservoirs. SPE J. 12 (5): 369-382. http://dx.doi.org/10.2118/3524-PA.
2. Cannella, W. J., Huh, C. and Seright, R. S. 1988. Prediction of Xanthan Rheology in Porous Media. SPE 18089 presented at the SPE Annual Technical Conference and Exhibition held in Houston, Texas, 2-5 October.
3. Carl Montgomery. 2013. Fracturing Fluid Components. http://dx.doi.org/10.5772/56422,.
4. Carreau, P. J. 1968. Rheological Equations from Molecular Network Theories. PhD dissertation, University of Wisconsin-Madison.
5. Chauveteau, G. and Kohler, N. 1984. Influence of Microgels in Polysaccharide Solutions on their Flow Behavior through Porous Media. Society of Petroleum Engineers Journal, May.
6. Delshad, M., Kim, D., Magbagbeola, O., Huh, C., and Pope, G.A. 2008. Mechanistic Interpretation and Utilization of Viscoelastic Behavior of Polymer Solutions for Improved Polymer-Flood Efficiency. SPE 113620 presented at the 2008 SPE Improved Oil Symposium held in Tulsa, Oklahoma, 19-23 April.
7. Economides, M. J., Nolte, K. J. “Reservoir Stimulation”. 2010, Third Edition.
8. Gall, B.L. and Raible, C.J. 1985. Molecular Size Studies of Degraded Fracturing Fluid Polymers. SPE 13566, Nat/. lnst. for Petroleum & Energy Research.
9. Hill, H.J., Brew, J.R., Claridge, E.L., Hite, J.R. and Pope, G.A. 1974. The Behaviour of Polymers in Porous Media. SPE 4748 presented at the Improved Oil Recovery Symposium of the Society of Petroleum Engineers of AIME, Tulsa, Oklahoma, USA.
10. Hirasaki, G.J. and Pope, G.A. 1974. Analysis of Factors Influencing Mobility and Adsorption in the Flow of Polymer Solution through Porous Media. Society of Petroleum Industry Journal, August.
11. Kelvin Nder Abba. 2016. Laboratory Investigation of Multiphase Permeability Evolution Due to Fracturing Fluid Filtrate in Tight Gas Sandstones. Dissertation, The Pennsylvania State University.
12. Maeker, J.M. and Sinton, S.W. 1984. Rheology Resulting from Shear-induced Structure in Associating Polymer Solutions. Journal of Rheology 30 (1): 077-099.

13. Nasr-El-Din, H. A., Al-Mohammed, A. M., Al-Aamri, A. D. and El-Fuwaires, O. A. 2007. A Study of Gel Degradation, Surface Tension and their Impact on the Productivity of Hydraulically Fractured Gas Well. SPE 109690-MS presented at SPE Annual Technical Conference and Exhibition, Anaheim, California, USA.
14. Nolte, K.G. 1982. Fracture Design Considerations Based on Pressure Analysis. SPE 10911 presented at the SPE Cotton Valley Symposium, Tyler, Texas, USA, May 20.
15. Sarwar, M.U., Cawiezel, K.E., and Nasr-El-Din, H.A. 2011. Gel Degradation Studies of Oxidatives and Enzyme to Optimize Breaker Type and Concentration for Effective Break Profiles at Low and Medium Temperature Ranges. SPE 140520.
16. Seright, R.S. 1983. The Effects of Mechanical Degradation and Viscoelastic Behavior on Injectivity of Polyacrylamide Solutions. Society of Petroleum Engineers Journal, June.
17. Todd, M. R. and Chase, C. A. 1979. A Numerical Simulator for Predicting Chemical Flood Performance. SPE 7689 presented at the SPE Reservoir Simulation Symposium, Denver, Colorado, 31 January-2 February. http//dx.doi.org/10.2118/7689-MS.
18. Weaver, J., Gdanski, R., and Karcher, A. 2003. Guar Gum Degradation: A Kinetic Study. Haliburton. SPE 80226.
19. Worlow, D.W. 1987. Development and Testing of a Standard Procedure for Determining the Viscous Properties of Crosslinked Fracturing Fluids. MS thesis, Texas A&M University, College Station, Texas, USA.
20. Worlow, D.W. and Holditch, S.A. 1989. Rheological Measurements of a Crosslinked Fracture Fluid Under Conditions Expected During a Fracture Treatment. SPE 18970 presented at the SPE Joint Rocky Mountain in Regional/ Low Permeability Reservoirs Symposium and Exhibition held in Denver, Colorado.
21. Zechner, M., Buchgraber, M. Clemens, T., Gumpenberger, T., Castanier, L. M., and Kovscek, A. R. 2013. Flow of Polyacrylamide Polymers in the Near-Wellbore-Region, Rheological Behavior within Induced Fractures and Near-Wellbore Area. SPE166085.

Tables

Table 1- Fracturing Fluids, Low Concentration Additives

Name	Fluid Type	Additives
Fluid 1	Linear Gel	20 pptg Guar
Fluid 2	Linear Gel	20 pptg Guar, 1 pptg Breaker
Fluid 3	Linear Gel with Surfactant*	20 pptg Guar, 1 pptg Breaker, 2 gptg Surfactant
Fluid 4	Crosslinked Gel	20 pptg Guar, 1 pptg Breaker, 2.5 gptg Crosslinker
Fluid 5	Crosslinked Gel with Surfactant	20 pptg Guar, 1 pptg Breaker, 2.5 gptg Crosslinker, 2 gptg Surfactant

Table 2- Fracturing Fluids, High Concentration Additives

Name	Fluid Type	Additives
Fluid 6	Linear Gel	40 pptg Guar
Fluid 7	Linear Gel	40 pptg Guar, 5 pptg Breaker
Fluid 8	Linear Gel with Surfactant	40 pptg Guar, 5 pptg Breaker, 3 gptg Surfactant
Fluid 9	Crosslinked Gel	40 pptg Guar, 5 pptg Breaker, 4 gptg Crosslinker
Fluid 10	Crosslinked Gel with Surfactant	40 pptg Guar, 5 pptg Breaker, 4 gptg Crosslinker, 3 gptg Surfactant

* non-ionic surfactant

Table 3-Input Data for Fracture Width Calculation

Fluid Pumping Rate, bbl/min	80
Fracture Height, ft	200
Young Modulus, psi	$1*10^6$
Poisson's Ratio	0.2

Formation Temperature, °F	120

Table 4- The Effect of the Fluid Thermal Degradation on the Fracture Width

Temp. °F	Fluid	Width Difference after 5 hours Inch
100	Fluid1	0.3
100	Fluid6	0.9
120	Fluids4 & Fluid5	0.85, 0.7
120	Fluids9 & Fluid10	>1
150	Fluids4 & Fluid5	>1
150	Fluids9 & Fluid10	>1

Table 5- Average Shear Rate in the Fracture, Temperature 100 °F

Fluid	Average Shear Rate after 1 hour Sec^{-1}	Average Shear Rate after 2 hours Sec^{-1}
Fluid1	450	200
Fluid4	120	90
Fluid5	90	50
Fluid6	1700	1000
Fluid9	700	400
Fluid10	600	350

Table 6- Average Shear Rate in the Fracture, Temperature 120 °F

Fluid	Average Shear Rate after 1 hour Sec^{-1}	Average Shear Rate after 2 hours Sec^{-1}
Fluid1	500	260
Fluid4	200	100
Fluid5	95	55
Fluid6	1800	1400
Fluid9	760	550
Fluid10	750	450

Figures

Figure 1– Fracturing Fluids Blender

Figure 2- Model 900 Viscometer

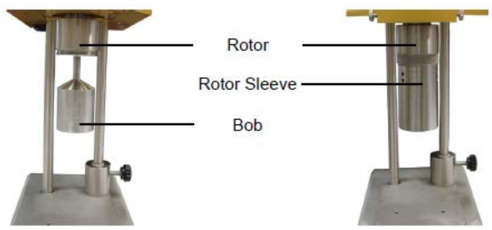

Figure 3- Geometry of the Cup & Bob

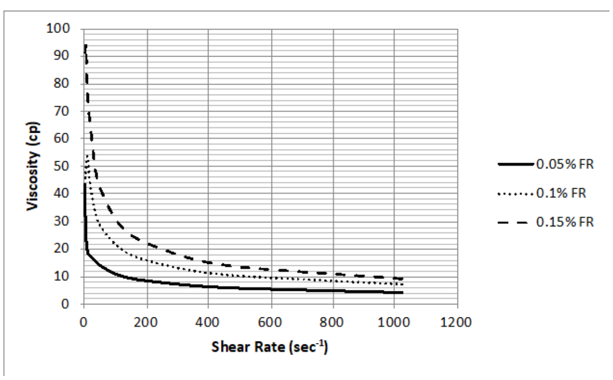

Figure 4- Apparent Viscosity vs. Shear Rate

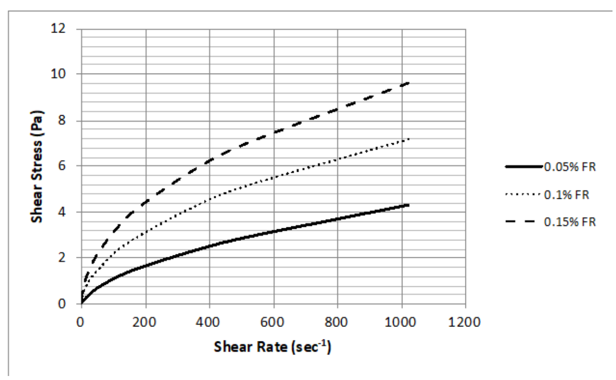

Figure 5- Shear Stress vs. Shear Rate

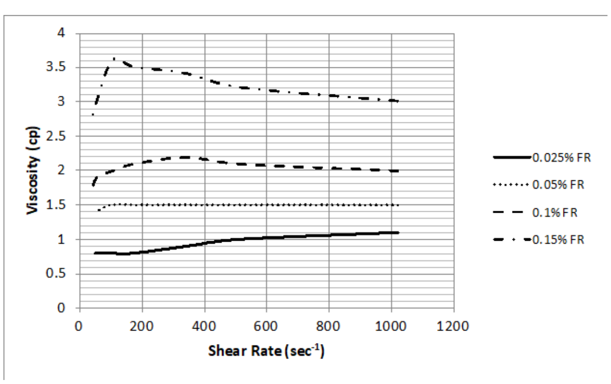

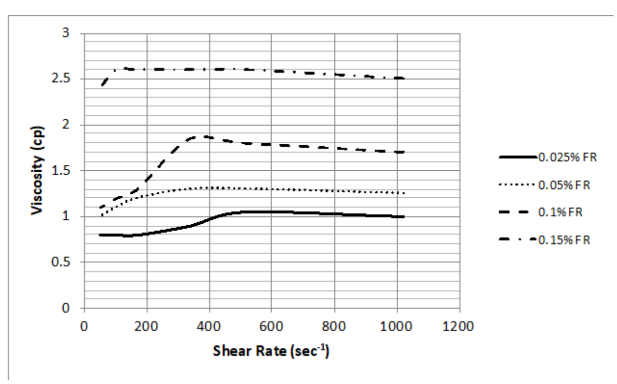

Figure 6- Viscosity vs. Shear Rate, KCl=1%

Figure 7- Viscosity vs. Shear Rate, KCl=3%

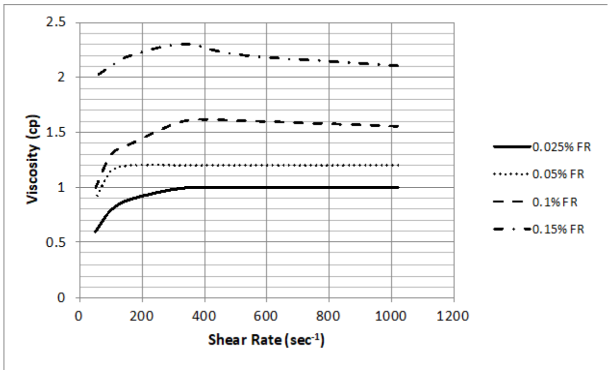

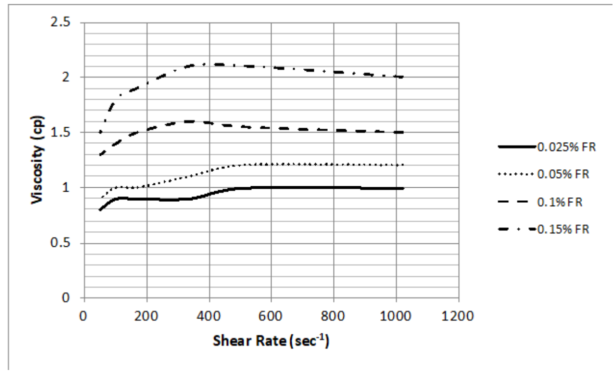

Figure 8- Viscosity vs. Shear Rate, KCl=5%

Figure 9- Viscosity vs. Shear Rate, KCl=7%

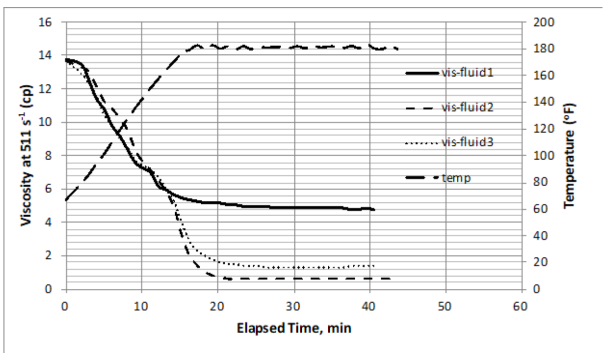

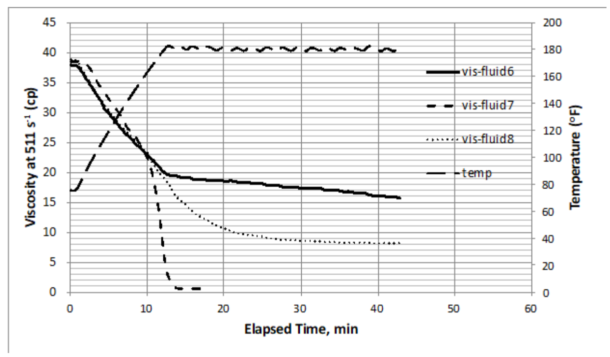

Figure10- Fluids Thermal Deg.- Group1- 180 °F

Figure 11- Fluids Thermal Deg.- Group2, 180 °F

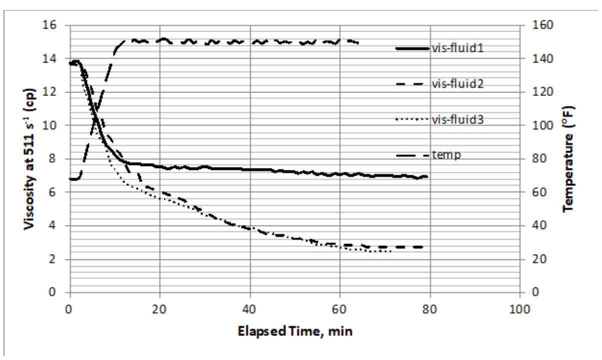

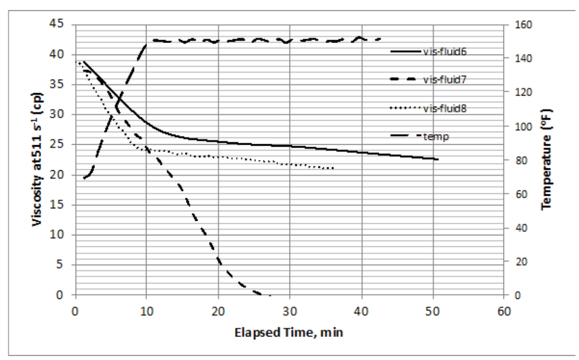

Figure 12- Fluids Thermal Deg.- Group1,150 °F

Figure 13- Fluids Thermal Deg.- Group2, 150 °F

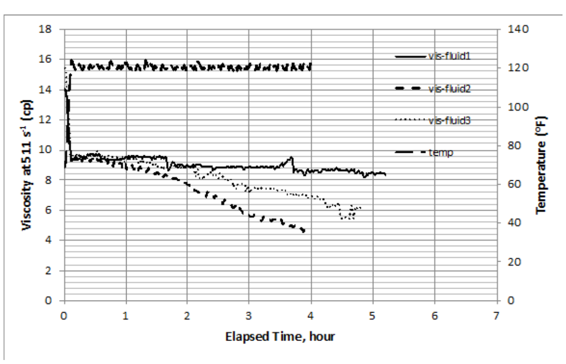

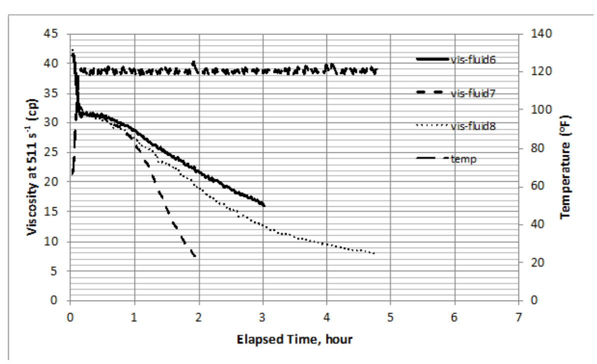

Figure 14- Fluids Thermal Deg.- Group1,120 °F

Figure 15- Fluids Thermal Deg., Group2, 120 °F

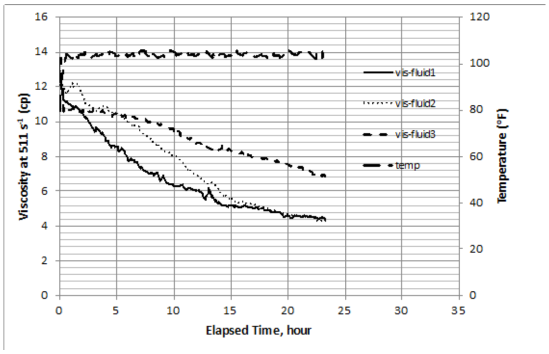

Figure 16- Fluids Thermal Deg.- Group1,100 °F

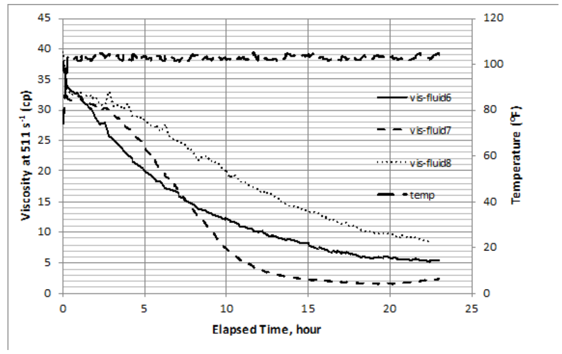

Figure 17- Fluids Thermal Deg., Group2, 100 °F

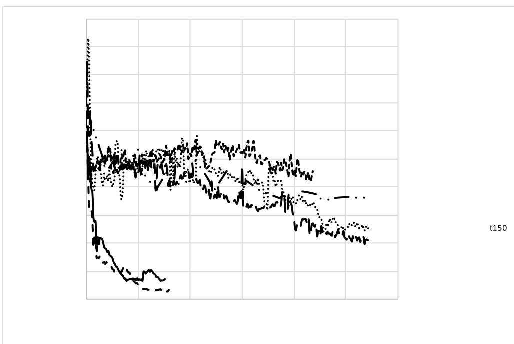

Figure 18- Fluids Thermal Deg.-Group1

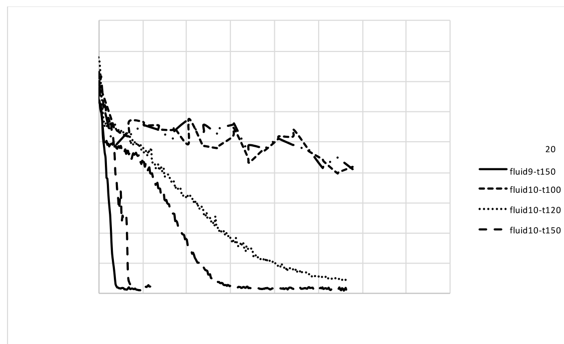

Figure 19- Fluids Thermal Deg.- Group2

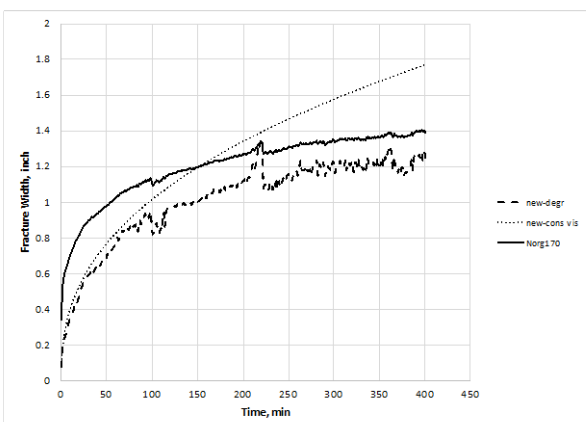

Figure 20- Fracture Width, Fluid1, Temp. 120 °F

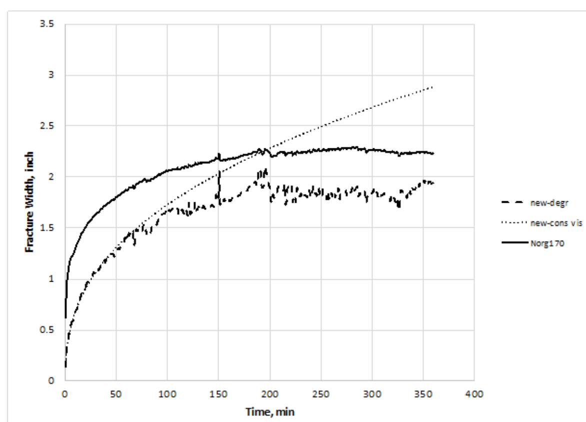

Figure 21- Fracture Width, Fluid4, Temp. 120 °F

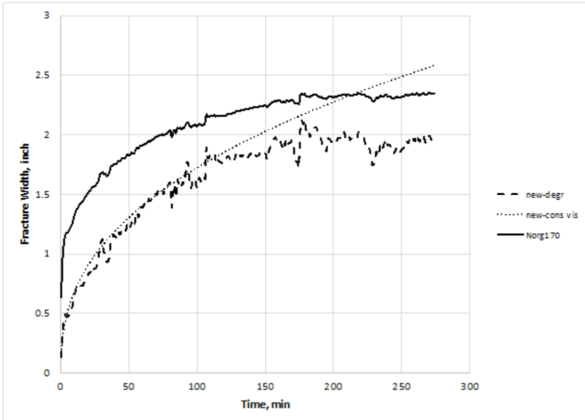

Figure 22- Fracture Width, Fluid5, Temp. 120 °F

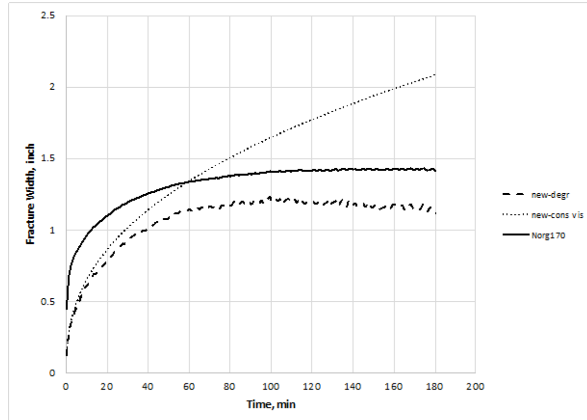

Figure 23- Fracture Width, Fluid6, Temp. 120 °F

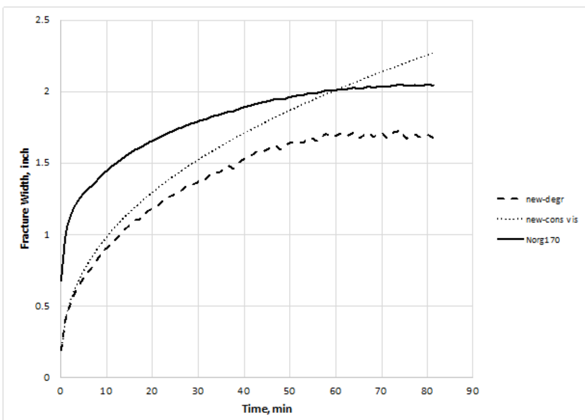

Figure 24- Fracture Width, Fluid9, Temp. 120 °F

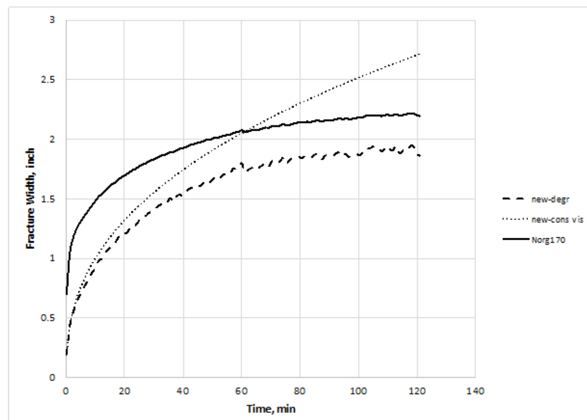

Figure 25- Fracture Width, Fluid10, Temp. 120 °F